Proceedings of Science and Mathematics
Faculty of Science, Universiti Teknologi Malaysia
Volume 33, 2026, page 71-84

Adsorption of Crystal Violet Dye onto Chlorine-Free Cellulose Derived from Oil Palm Empty Fruit Bunch

Nurul Syafiqah Bahari[a], Nurrulhidayah Salamun[a]*
[a]Department of Chemistry, Faculty of Science, Universiti Teknologi Malaysia, 81310 UTM Skudai, Johor, Malaysia
*Corresponding author: nurrulhidayah@utm.my

Abstract
A green approach in extraction of cellulose derived from oil palm empty fruit bunch (OPEFB) by using chlorine free hydrolysis method offer a great potential in synthesizing an eco-friendly adsorbent. OPEFB is the most abundant plantation effluent, containing cellulose (40%-50%), hemicelluloses (20%-30%), and lignin (15%-20%). In this study, two methods; bleaching and non-bleaching methods were carried out on the fibres of OPEFB to differentiate the efficiency of the two methods in producing cellulose and to determine if the chlorine free hydrolysis method can be a substitution method to bleaching method which is less environmentally friendly. The cellulose produced were named as cellulose-sodium chlorite (C-SC) and cellulose-hydrogen peroxide (C-HP). As for chlorine free hydrolysis method, the ATR-FTIR spectra showed peaks at 3330.58 cm^{-1} and 2894.97 cm^{-1} which attributed to –OH and C-H groups stretching vibrations. Based on the XRD diffractogram, the crystallinity index (C_I) obtained for C-SC and C-HP were 44.66% and 37.85%, respectively. This result illustrated that the chlorine free hydrolysis treatments affected an improvement in the crystallinity of the cellulose. The high crystallinity values of the C-HP can be attributed to the efficient removal of the non-cellulosic components of the fibres by the non bleaching treatments. TGA results showed that the C-HP starts to degrade thermally at 352˚C meanwhile the C-SC starts to decompose at 366˚C. The adsorption of crystal violet (CV) onto C-HP showed a higher adsorption uptake with 83.46 mg/g as compared to C-SC with just only 43.18 mg/g. When varying the pH of the CV solution, pH 8 was revealed to be the best pH condition for adsorption of CV onto C-HP.
Keywords: chlorine-free hydrolysis; cellulose OPEFB; adsorption

Introduction

The discharge of dye-containing industrial wastewater poses a serious threat to aquatic ecosystems and water quality worldwide. Dyes are extensively used in industries such as textiles, paper and pulp, dye manufacturing, food processing, electroplating, and distilleries, leading to the release of large volumes of coloured effluents into water bodies (Xing et al., 2010). It has been estimated that over 280,000 tonnes of textile dyes are discharged into the environment annually, with the majority entering aquatic systems (Shertate et al., 2013). Due to their complex aromatic structures, many dyes are resistant to biodegradation and can exhibit toxic or carcinogenic effects, necessitating effective wastewater treatment strategies.

Among the available treatment technologies, adsorption is widely recognised as one of the most efficient and practical methods for dye removal. Adsorption enables the elimination of dye molecules without generating harmful degradation by-products and is favoured for its operational simplicity, energy efficiency, and cost-effectiveness (Dotto et al., 2012). The process involves the accumulation of dissolved contaminants on the surface of a solid adsorbent through intermolecular interactions and is extensively applied in industrial wastewater treatment (Vital et al., 2016). Although conventional adsorbents such as activated carbon and zeolites are effective, their high cost and limited sustainability have driven the search for low-cost, renewable alternatives.

Cellulose has emerged as a promising natural adsorbent due to its abundance, biodegradability, and global availability as a renewable polymer resource. Numerous studies have explored cellulose-based materials as environmentally friendly substitutes for non-renewable and expensive adsorbents (Yin Ng et al., 2020). Structurally, cellulose is a linear polysaccharide composed of β-(1→4)-linked anhydroglucose units with the molecular formula $(C_6H_{10}O_5)_n$. The presence of reducing and non-reducing end groups contributes to its chemical stability (Klemm et al., 2005). However, native cellulose is insoluble in water and often requires chemical modification or purification to enhance its functional performance (Liesiene et al., 2013).

Malaysia's oil palm industry generates vast quantities of lignocellulosic waste, particularly Oil Palm Empty Fruit Bunches (OPEFB). Approximately 19.8 million tonnes of OPEFB are produced annually on a wet basis, equivalent to 6.93 million tonnes on a dry basis (Foo et al., 2011). OPEFB consists mainly of cellulose (40–50%), hemicellulose (20–30%), and lignin (15–20%), making it an attractive feedstock for sustainable cellulose extraction. Structurally, OPEFB comprises crystalline cellulose embedded within an amorphous matrix of hemicellulose and lignin. To obtain high-purity cellulose from OPEFB, chemical pretreatment and bleaching are required to remove non-cellulosic components. Conventional bleaching methods often rely on chlorinated reagents, which have raised environmental concerns due to the formation of toxic organochlorine compounds (Tarchoun et al., 2019). As a result, chlorine-free and environmentally benign bleaching systems have gained increasing attention, including the use of hydrogen peroxide and organic acids (Beroual et al., 2021). Hydrogen peroxide is particularly attractive due to its strong oxidative capability, rapid delignification efficiency, and environmentally friendly decomposition into water and oxygen. Its bleaching mechanism involves reactive free radicals and perhydroxyl anions, enabling the effective removal of lignin and hemicellulose in a single step (Zeronian et al., 1995; Song et al., 2019).

In this study, a green and chlorine-free approach is proposed for the extraction of cellulose from OPEFB using a hydrogen peroxide–acetic acid system. This method employs low reagent concentrations, mild operating conditions, and reduced energy input, while allowing easy recovery of acetic acid after delignification (Li et al., 2012). The extracted cellulose is characterised using Fourier Transform Infrared Spectroscopy (FTIR), Thermogravimetric Analysis (TGA), and X-ray Diffraction (XRD) to evaluate its functional groups, thermal stability, and crystallinity. The work aims to valorise OPEFB waste into a sustainable cellulose material with potential application as a low-cost adsorbent for dye removal from wastewater.

Materials and methods

Preparation of Empty Fruit Bunch

OPEFB fibers were blended by using a grinder and then washed with distilled water three times. After washed, the collected fibers were placed in a dry oven for 24 hours and at 80oC. The weight of dry fibers was taken and after that was mixing with chemical toluene and ethanol for six hours. Then, the dry fibers were put again in the dry oven for 24 hours, at 80˚C.

Digestion of Empty Fruit Bunch

The empty fruit bunch was digested with (1.0M) NaOH at 80˚C for 4 hours. Then the solution was prepared (10g/250mL) and wash with distilled water until pH 7 (neutral). Then, the fibre was undergoing bleaching process with sodium chlorite ($NaClO_2$).

Bleaching Treatment

Bleaching of fiber is effective at removing surface impurities, lignin and hemicellulose, thereby producing brighter color and rougher fiber surface which promotes fiber/matrix adhesion as depicted by SEM micrographs (Rayung et al, 2014).

Hydrolysis with Weak Acid

The fibres were soaked in a solution of 20% acetic acid and 10% hydrogen peroxide and placed in an 85 °C water bath for two hours. The fibres were then washed again with 10% acetic acid and then with distilled water. Cellulose was extracted in a light yellow colour. Finally, the extracted cellulose was resuspended in 10% hydrogen peroxide and 10% sodium hydroxide and heated to 60°C for 90 minutes to obtain white cellulose. Then, collected the extracted cellulose (Jahan et al. 2011). The cellulose

produced were named as cellulose-hydrogen peroxide (C-HP).

Bleaching with $NaClO_2$

The fibres were bleached with 1.3% sodium chlorite and 10% acetic acid. The fibres were then washed with NaOH (0.1M) and distilled water until reached pH of 6-7. Then, the extracted cellulose was placed in the dry oven for 24 hours and final weight was recorded. The cellulose produced were named as cellulose-sodium chlorite (C-SC).

Characterizations

The adsorbent, extracted cellulose were characterized by TGA, ATR-FTIR and XRD in order to determine the morphology of the cellulose, to determine its significant functional group and to determine the crystallinity of the product respectively.

Thermogravimetry Analysis (TGA)

TGA (Pyris 1, Perkin Elmer) was used to investigate the thermal stability of raw OPEFB and extracted cellulose. In a nitrogen atmosphere, ten mg of material (dry) was kept under TGA observation at a predetermined temperature range of 30 to 700 ˚C. Before the samples were run, a continuous nitrogen flow of 30 cm^3min^{-1} was maintained, followed by a furnace flow rate of 150 cm^3min^{-1}.

X-Ray Diffraction (XRD)

XRD pattern was recorded using Bruker D8 advance, equipment. The isolated cellulose was scanned in the range of 2θ = 5° to 90° at a step time of 0.2 s/step at 25 °C with Cu kα radiation, λ = 0.1540 nm. The crystallinity index (C_I) of dried cellulose was determined using the equation (1) (Ling, et al, 2019).

$$C_I\,(\%) = \frac{A(crystalline) - A(amorphous)}{A\,(crystalline)}\, x\ 100\% \qquad (1)$$

Attenuated Total Reflectance Infrared (ATR-IR)

Attenuated Total Reflectance-Fourier Transmission Infrared Spectroscopy (ATR-FTIR) studies was performed using a PerkinElmer spectrophotometer to determine the functional group of the chlorine-free cellulose. ATR-FTIR was performed with the wavenumber range of 4000-500 cm^{-1} and the resolution of 4 cm^{-1} at an accumulation of 32 scans.

Absorption of Crystal Violet onto Cellulose

To study the adsorption of the chlorine-free cellulose and crystal violet, there are several factors that will be investigate which is effect of contact time, effect of pH, and effect of concentration. Throughout the experiment, only one parameter will be adjusted to the desired value while the others parameter will remain constant.

The effect of contact time, the time dependency was planned at pH 6, adsorbent dosage of 1.5g/50mL and temperature at 35ºC process condition as maximum adsorption was attained at these levels. The effect of contact time was correlated for the adsorption of crystal violet ions at regular time intervals ranging from 5 min. to 180 min. Next, the range for effect of pH will be investigated from 2 to 8. The range for the effect of initial concentration are 50 mg/L to 250 mg/L on adsorption was investigated under specified conditions (pH 8, dosage 1.5g/50mL, room temperature, contact time 90 min.) (Gnanasundaram et al, 2016).

Adsorption Isotherm

Adsorption isotherm models are commonly employed to interpret equilibrium data and to elucidate the interaction mechanisms between an adsorbate and an adsorbent during the adsorption process. In the present study, the equilibrium behaviour of dye adsorption was analysed using two widely applied isotherm models, namely the Langmuir and Freundlich models, to describe the distribution of dye ions between the solid adsorbent and the aqueous phase at constant temperature.

The Langmuir isotherm model is based on the assumption that adsorption occurs on a homogeneous surface with a finite number of identical and energetically equivalent active sites.

According to this model, each adsorption site can accommodate only one dye molecule, leading to monolayer coverage without lateral interactions between adsorbed species (Langmuir, 1917). Once an active site is occupied, no further adsorption can take place at that site. The linear form of the Langmuir isotherm is expressed as equation (2):

$$\frac{C_e}{q_e} = \left(\frac{1}{K_L q_m}\right)\left(\frac{1}{C_e}\right) + \frac{C_e}{q_m} \qquad (2)$$

where q_e (mg g^{-1}) represents the amount of dye adsorbed at equilibrium, C_e (mg L^{-1}) is the equilibrium concentration of dye in solution, q_m (mg g^{-1}) denotes the maximum monolayer adsorption capacity, and K_L (L mg^{-1}) is the Langmuir adsorption constant related to the affinity of the binding sites. In contrast, the Freundlich isotherm model describes adsorption on a heterogeneous surface with a non-uniform distribution of adsorption energies and allows for multilayer adsorption. This empirical model also accounts for interactions between adsorbed molecules (Freundluich, 1906). The linear form of the Freundlich isotherm is given by equation (3):

$$log\ q_e = ln\ K_f\ + \frac{1}{n} log\ C_e \qquad (3)$$

where K_f ($L^{1/nf}$ $mg^{(1-1/nf)}$ g^{-1}) is the Freundlich constant indicative of adsorption capacity, and 1/n is the Freundlich heterogeneity factor that reflects the adsorption intensity and surface heterogeneity.

Results and discussion

Chemical Composition of Fibres

Pre-treatment is one of the most important processes before extracting cellulose from the fibre. Prior to further treatment, the major goal of the pretreatment procedure is to degrade the lignin structure, reduce cellulose crystallinity, and raise the porosity of the lignocellulosic materials. In this study, C-HP were extracted by chlorine-free hydrolysis method using hydrogen peroxide (H_2O_2) from oil palm empty fruit bunch (OPEFB) that changed brown OPEFB into the cellulose-rich creamy white pulp. Only 1 wt% of cellulose solid was used in the processing since nanofibrillation involves the breakage of hydrogen bonds in between cellulose microfibrils which eventually caused the nanocellulose to have very high-water holding capacity, and hence a thick, gel-like cellulose suspension in water will be produced (Liana Noor Megashah et al., 2018). The fibres were treated with 4% w/v NaOH solution for the removal of hemicellulose. The intermolecular ester bond between carbohydrate and lignin is broken down due to the alkaline conditions (Johar et al., 2012). NaOH is used to increase the yield of cellulose during the pulping process since NaOH increases accessibility of the core material for hydrolysis action, which makes NaOH acts as a pre-swelling agent (Jonoobi et al., 2011). It was found that there were significant changes in the content of cellulose, hemicellulose, and lignin when undergo the chlorite treatment and chlorine-free hydrolysis.

Table 1: Comparison of extracted cellulose in two different bleaching reagents.

Sample Composition	C-HP (%)	C-SC (%)
Cellulose	72.2	72.1
Hemicellulose	24.0	17.5
Lignin	4.8	10.4

These findings show that the bleaching procedure is significant in removing both hemicellulose and lignin at the same time. According to the chemical composition analysis in Table 1, chlorite bleaching effectively removed the majority of the hemicellulose and lignin from OPEFB with 72.1% (w/w). The alkali treatment procedure eliminates only a little amount of hemicellulose from the treated fibre (Rosli *et al.,* 2013). The final stage of chlorine-free hydrolysis for 2 hours reduced the amount of lignin and hemicellulose fraction by a small amount. On a dry weight basis, the cellulose yield from this treatment was 72.2% (w/w). The cellulose content was higher than that reported by other researchers, which differed from 44.4% (Sun *et al.* 1999), 60.6% (Wanrosli *et al.* 2004), 49% (Nazir *et al.* 2012) and 64% (Nazir *et al.* 2013). It is possible that the difference in cellulose content is attributable to the varied

origins and hydrolysis conditions (De Menezes *et al.* 2009; Li *et al.* 2009).

Chlorinated organic molecules are produced in huge quantities as a result of conventional bleaching techniques that use chlorine and chlorine derivatives, causing serious environmental hazards. Chlorite (ClO_2^-) in acidified sodium chlorite ($NaClO_2^+ H_3O^+$) forms a chlorine radical, Cl, which reacts and breaks the lignocellulosic material producing extremely poisonous organochlorine (Nazir *et al.*, 2013). As a result, the use of chlorine-free bleaching processes has gained much importance. The hydroperoxide anion (HOO^-), which is dominantly present in alkaline circumstances and responsible for the removal of chromophoric groups from lignin, is responsible for chlorine-free hydrolysis using hydrogen peroxide (Shahi *et al.*, 2020). One of the green approaches that has been investigated is Haverty et al earlier.'s study on autothermal degradation of Miscanthus x giganteus to cellulose fibre using hydrogen peroxide. According to Nazir et al., cellulose fibres recovered from the OPEFB using hydrogen peroxide and an ultra-assisted alkali extraction produce 49% cellulose. The morphological, structural, and chemical features of the obtained gel-like cellulose suspensions were analysed and are discussed below.

Characterization of Raw OPEFB, C-HP, and C-SC

Thermogravimetry Analysis (TGA)

The initial weight loss for the first breakdown is ascribed to the loss of water content and volatile substance at temperature for the first 300˚C, according to the results obtained. The cellulose is thermally degraded in the second composition. Due to moisture evaporation or breakdown of the low molecular weight chemicals, weight loss changed slightly at lower temperatures (below 100˚C) (Sheltami et al. 2012; Mohamad et al. 2013). Figure 1 shows the thermogravimetric curves of raw OPEFB, C-HP, and C-SC. The raw OPEFB had a greater weight loss from 30 to 650˚C compared to the C-HP fiber and C-SC fiber. According to Jonoobi et al. (2011), lignocellulosic materials begin to degrade thermally with hemicelluloses, followed by lignin pyrolysis, cellulose depolymerization, and char oxidation. Thus, raw OPEFB fiber with high amount of hemicellulose and lignin showed or higher weight loss compared to C-SC samples that had been treated with chlorite bleaching. C-HP shows a lower thermal degradation after 270˚C compared to both raw OPEFB. This might be due to the low duration of chlorine-free hydrolysis, which had led to deterioration of thermal stability of the cellulose.

According to the Table 2, the weight loss of the samples is related to the thermal degradation of hemicellulose, cellulose and lignin. for OPEFB – RAW shows the thermal degradation at temperature 250˚C due to the reflection on the decomposition temperature of lignin and hemicellulose. For the OPEFB – C the thermal degradation occurs at 225˚C which correspond to the decomposition of the cellulose. For C-HP the thermal degradation occurs at 272˚C at this temperature the cleavage of glycosidic linkages of cellulose was occurred. Major weight loss for C-HP occurred around 352˚C contributed by the degradation of cellulose and weight loss of lignin.

Table 2: Thermogravimetric data of raw OPEFB, raw cellulose, C-HP and C-SC.

Sample	IDT (˚C)	DT (˚C) at every 10% weight loss						Residue Left (%)
		20	30	40	50	60	70	
Raw OPEFB	250	300	325	350	365	545	600	33
Raw Cellulose	225	290	320	340	350	530	585	30
C-HP	275	281	311	328	348	520	637	31
C-SC	281	352	391	431	463	509	531	28

X-Ray Diffraction (XRD)

Figure 2 demonstrates XRD angle patterns of raw OPEFB, C-HP and C-SC in the range 2θ of 0˚- 65˚. OPEFB fibres are made up of amorphous (hemicellulose, lignin) and crystalline (cellulose) structures in their natural state. Since the cellulose fibres may still be entrapped in amorphous hemicellulose and lignin, the peak intensity is low. The identity and character of a substance can be determined using the X-Ray Diffraction (XRD) pattern. The pattern of crystallinity and amorphous levels in cellulose can be determined (Osvaldo et al., 2012). Cellulose fiber with a high crystallinity index assessed is defined as having the best concentration. The higher the crystallinity index, the sharper the peak. According to the XRD diffractogram, the crystalline indexes of each isolated cellulose were 21.35%, 44.66%, and 37.85% for raw OPEFB, C-HP, and C-SC respectively.

Higher crystallinity is achieved by removing nanocellulosic polysaccharides and dissolving amorphous regions (Ismail et al., 2021). The highest crystalline index was obtained by polymer a hydrogen peroxide acid concentration of 10% v/v. This means that this concentration is ideal for extracting cellulose derived from OPEFB. Raw OPEFB was found to have a broad and high-intensity XRD diffractogram pattern at 2θ = 22.7˚. However, after the 10% concentration of hydrogen peroxide hydrolysis procedure, two primary peaks with high intensities formed at 2θ = 23.07˚, which is a characteristic peak of the cellulose crystalline lattice. This indicates that hemicellulose epolymerization and delignification were completed satisfactorily (Nazir et al., 2013).

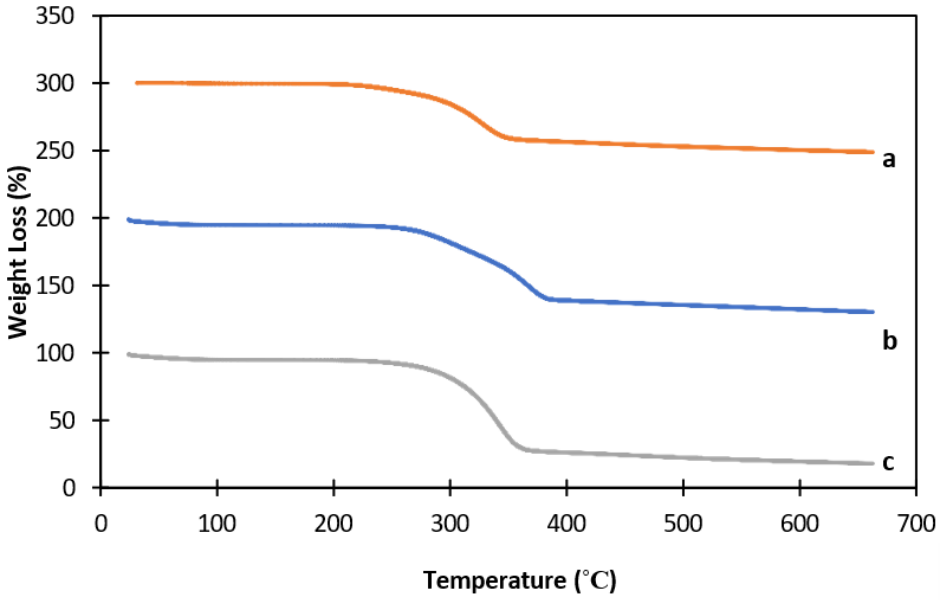

Figure 1 TG curves of (a) C-HP. (b) raw OPEFB and (c) C-SC.

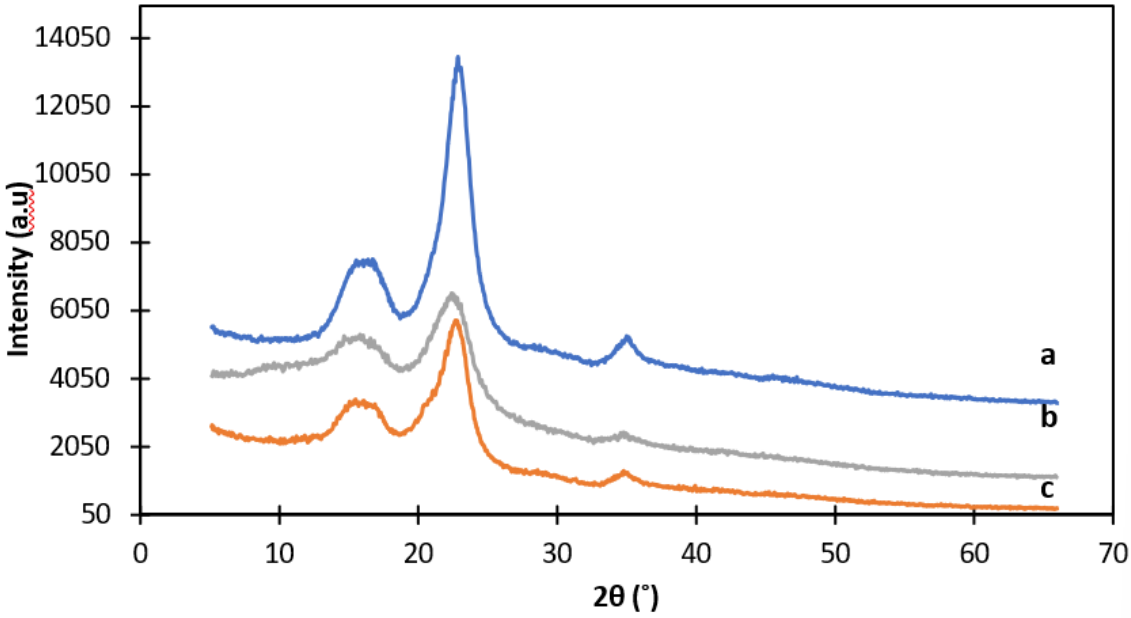

Figure 2 Diffraction angle XRD patterns of (a) C-HP (b) raw OPEFB and (c) C-SC.

Attenuated Total Reflectance Infrared (ATR-IR)

FTIR characterization has been widely and extensively employed in characterizing cellulose. It provides a useful information regarding the chemical structure changes in the sample, especially lignocellulosic. Figure 3 show the FTIR spectra of raw OPEFB, C-HP and C-SC respectively. Table 3 shows peaks of both spectra with similar functional groups.

According to the Table 3, the chemical compositions of the samples changed a little after the chlorine- free hydrolysis treatment. The peaks at 3332.05, 3331.23 and 3330.58 cm^{-1} are due to O-H stretching, which is caused by the vibration of hydrogen linked to the hydroxyl group. The lignin polysaccharide (cellulose and hemicelluloses) exhibits vibrational stretching in the form of saturated aliphatic C-H at 2891.65 cm^{-1}, 2895.82 cm^{-1} and 2894.97 cm^{-1}. The occurrence of a broad band about 3700-3100 cm^{-1}, which shows the presence of the O-H group in their primary component, reflects the tendency of hydrophilic fibre before hydrolysis and cellulose fiber. Because of the strong interaction between cellulose and water, transmittance bands around 1636.14 cm^{-1}, 1638.64 cm^{-1} and 1633.31 cm^{-1} were assigned to absorb water.

Table 3: Peaks of spectra raw OPEFB, C-SC and C-HP.

Raw OPEFB (cm^{-1})	C-SC (cm^{-1})	C-HP (cm^{-1})	Functional Groups
3332.05	3331.23	3330.58	O-H stretching vibration
2891.65	2895.82	2894.97	C–H stretching vibration
1636.14	1638.64	1633.31	Water absorption
1160.95	1158.38	1159.61	CH rocking vibration
1324.55	1367.55	1367.68	C-H bending vibration
1031.36	1027.29	1029.41	C-O-C pyranose
897.37	896.65	897.34	β-glycosidic linkage

The O-H bending of the adsorbed water was recognized to identify the transmittance peaks exhibited in both spectra at around 1640 cm^{-1}. The absorption of moisture in the areas left vacant from the elimination of lignin and hemicellulose could explain the moisture content. The open surfaces created by the alkali treatment cellulose aid in moisture absorption. Furthermore, chlorine-free hydrolysis results in the formation of hydroxyl groups on the surface of cellulose. The bending vibration of the C-H and C- O bonds in the polysaccharide aromatic rings are related to the vibration peak identified at 1324.55 cm^{-1}, 1367.55 cm^{-1} and 1367.68 cm^{-1} in cellulose OPEFB.

The presence of cellulose, which is known as β-glycosidic linkages between the sugar units can be seen around the peak 897.37 cm-1, 896.65 cm-1 and 897.34 cm-1. As the hydrolysis period was extended, the spectra of hydrolysis sample (C-HP) grew shallower than the unhydrolysis sample (raw OPEFB) at peaks around 3300-3500 cm-1. Hydrogen bonds were broken down as a result of chlorine- free hydrolysis. FTIR has also detected for the presence of lignin and hemicellulose in the raw OPEFB, C-HP and C-SC. It is assumed that due to its complex structure, it is difficult to remove lignin and hemicellulose fully from the plant biomass. Figure 4.3 showed.

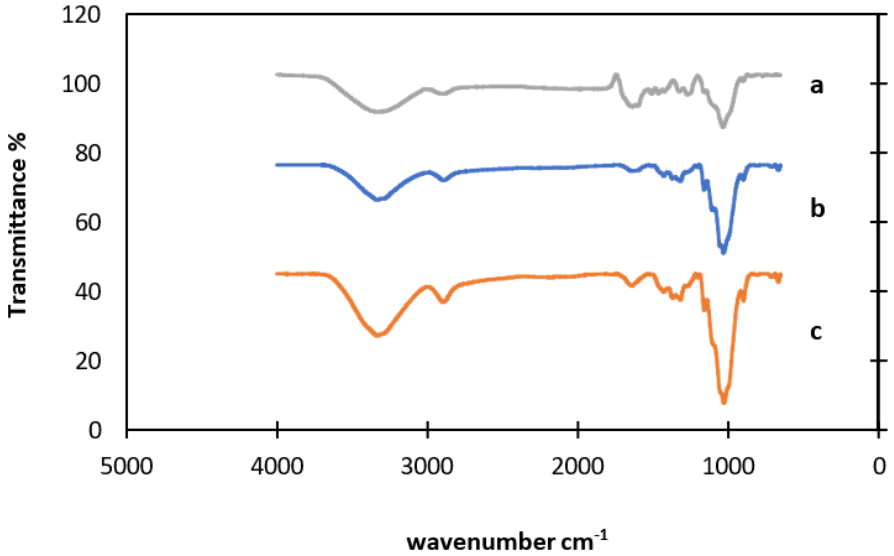

Figure 3 ATR-FTIR spectra of (a) raw OPEFB (b) C-HP and (c) C-SC.

Adsorption Uptake of Crystal Violet onto C-HP

Effect of Contact Time

The impact of contact time on the removal CV using C-HP and C-SC are shown in Figure 4. The rate of adsorption of CV was determined by using 10 mgL^{-1} of dye solution at pH 6, at room temperature with 0.02 g of adsorbent for each C-HP and C-SC for different interval of time range from 5 min until 180 min. The equilibrium (sorbate-sorbent contact) was reached within 180 min. The uptake of dye occurs in two stages; the first stage is a rapid uptake during 30 min, trailed by slow stage over a longer period (> 60 min) until the equilibrium was reached. The sample was taken 5ml each interval of time and put into the vial. The high rate of expulsion in the first stage was attributable to the large surface area exposed for CV adsorption. Due to the repulsive attraction between the solute molecule and the bulk phase, the adsorbent's capacity is eventually depleted, and there are few empty sites left in the adsorption process (Wanyonyi et al.2014). Based on the results, C-HP produced high value in adsorption uptake compared to C-SC, so C-HP was chosen to be an adsorbent for the next parameter of pH in time interval 90 min.

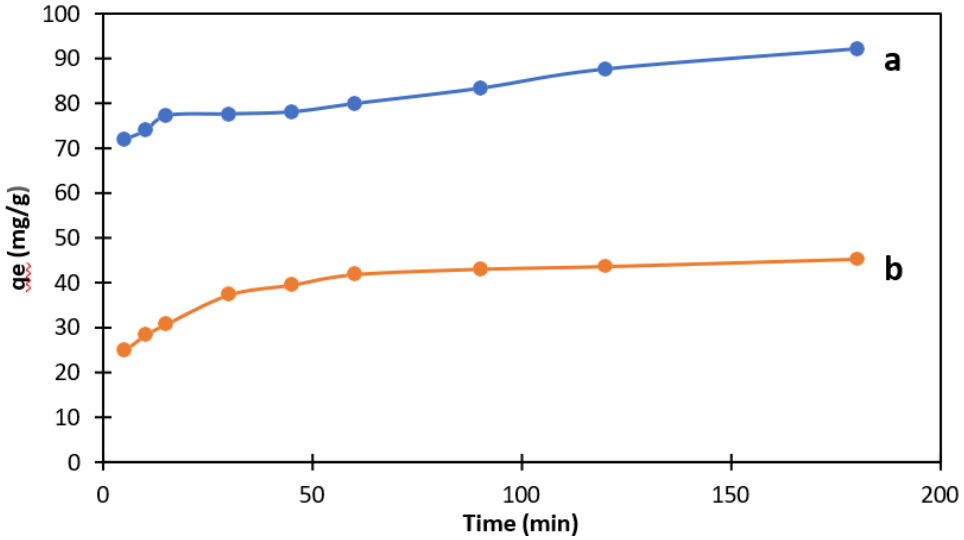

Figure 4 Effect of contact time on adsorption of CV onto (a) C-HP and (b) C-SC.

Effect of pH

pH is a key parameter that influences the adsorption process due to its effects on surface charge of adsorbent, degree of dissociation and ionization of dye molecule (Chakraborty et al. 2011). Figure 5 shows the adsorption capacity of CV dye was calculated at different pH (2, 4, 6 and 8) using 10 mg L^{-1} of dye, adsorbent dose of 0.02 g for 90 min at room temperature. At low pH, the removal of CV was low due to protonation of surface functional group of cellulose and become positively charged. The electrostatic repulsion between the surface of cellulose and positively charged dye declines the removal. In addition, hydrogen ions compete with the cationic group of the dye molecule for sorption site of adsorbent. The adsorption increases at higher pH because of the deprotonation of charged group present in the surface of adsorbent. This leads to electrostatic attraction between the positively charged group in the dye and negatively charged surface, supporting the adsorption process (Chakraborty et al. 2011).

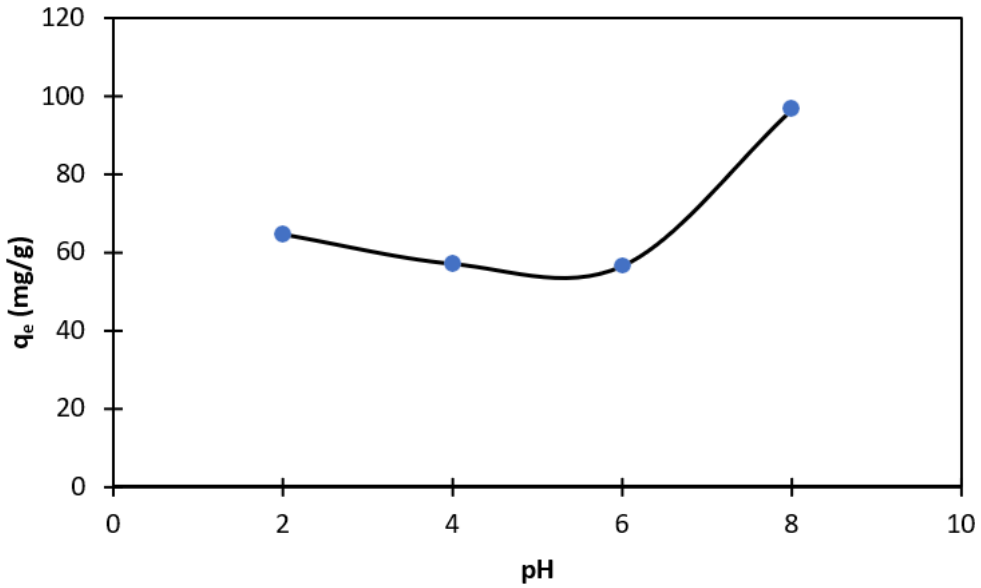

Figure 5 Effect of pH on adsorption of CV onto C-HP.

Effect of Initial Concentration

The adsorption capacity of CV was resolved at different concentrations (10, 50, 80, 100, 200, 250 mg L−1) at room temperature using 0.02 g of adsorbent at pH 8 for 90 min. The impact of various concentration of CV dye on removal is displayed in Figure 6. The removal diminishes with increasing dye concentration due to the saturation available active site of adsorbent.

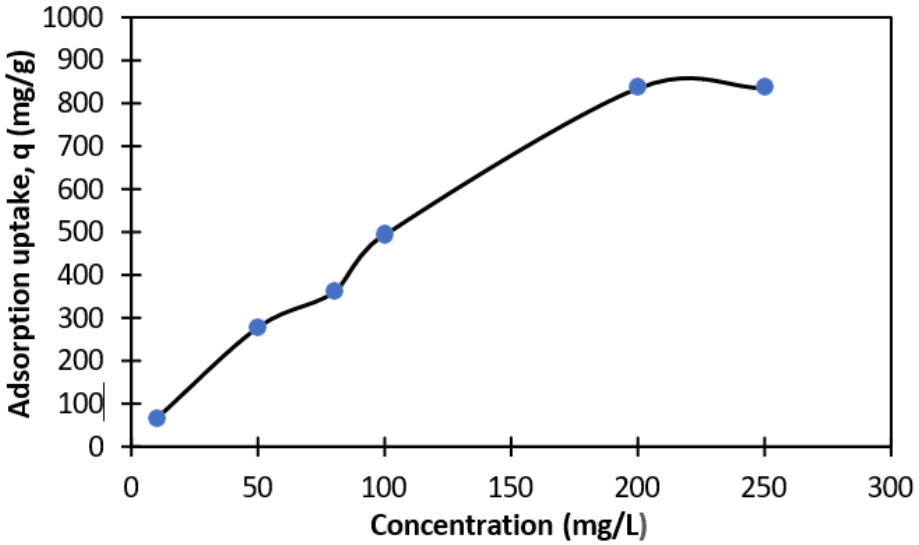

Figure 6 Effect of concentration on adsorption of CV onto C-HP.

Adsorption Isotherm

The adsorption isotherm was evaluated at different concentration, by keeping pH 8, room temperature and the adsorbent weight of 0.02g. Adsorption equilibrium data were evaluated by Langmuir and Freundlich isotherm model. Where C_e is the concentration at equilibrium (mg L^{-1}) and q_e is the adsorption capacity at equilibrium (mg g^{-1}).

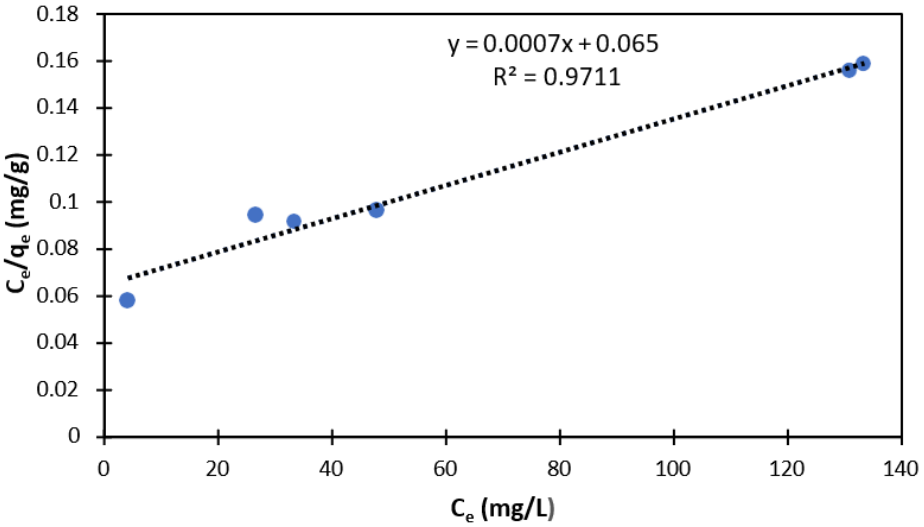

Figure 7 The Langmuir isotherm plots for the adsorption of CV onto C-HP at different CV ions concentration.

Freundlich isotherm model is given by equation, where k*f* (Freundlich constants) is an indicator of the adsorption capacity related to binding energy (mg g^{-1}), n is a Freundlich isotherm constant that measure adsorption intensity or surface heterogeneity (Wanyonyi et al.2014). Plotting ln qe versus ln Ce is shown in Fig.4.8 giving linear relationship in CV adsorption and R^2 of CV adsorption. From this result, adsorptions of CV on cellulosic adsorbent follow the Freundlich isotherm model. The value of n indicates a strong interaction between sorbent and solute molecule; it also indicates favorable sorption.

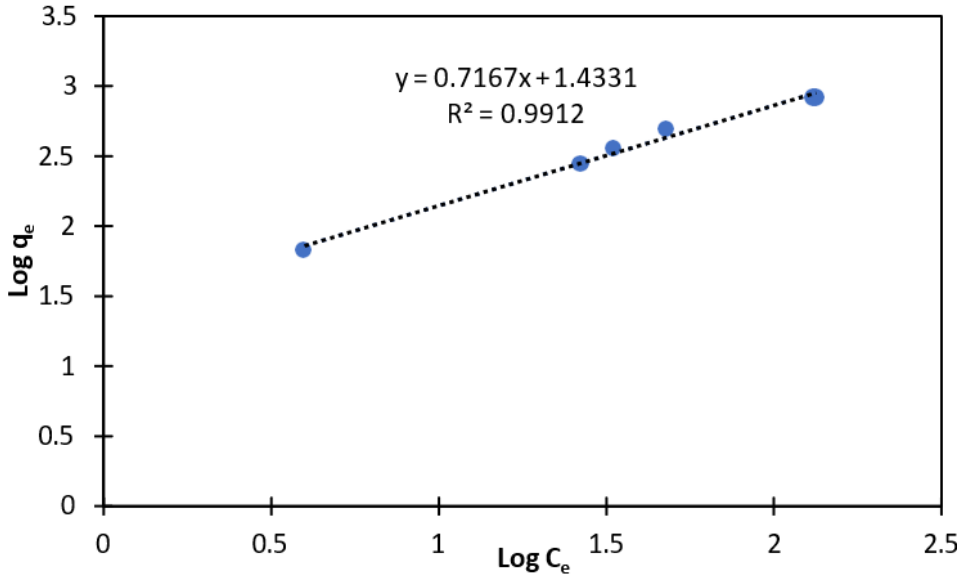

Figure 8 The Freundlich isotherm plots for the adsorption of CV onto C-HP at different CV ions concentration.

The q_m value evaluated from Langmuir isotherm for adsorption of CV was slightly higher than other studies stated in Table 4, indicates that the prepared C-HP is relatively more efficient as an adsorbent for CV removal. The experimental data for CV adsorption fitted well with Freundlich isotherm with R = 0.9912 and the np value of this model obtained was 1.395 which is in range of $0 < 1/ny < 1$ indicates favorable adsorption of CV dye at experimental conditions. Furthermore, this model shows the best fit to the experimental data due to the lowest MPSD value (MPSD = 0.927) compared to other isotherm models. The Freundlich model describes multilayer adsorption isotherm, assuming that the distribution of adsorption sites on the adsorbent surface is heterogeneous (Zhang et al., 2019). Based on the experimental fitting data, the best isotherm model fitted for CV adsorption on C-HP was Freundlich isotherm model.

Table 4: Parameters of the adsorption isotherm models.

Langmuir Isotherm		
q_m (mg/g)	K_L (L/mg)	R^2
1428.571	0.0108	0.9711
Freundlich Isotherm		
n	K_F (L/g)	R^2
1.395	27.108	0.9912

Comparison with Other Adsorbents

In order to evaluate the adsorption performance of C-HP, it is important to determine its position compared with other adsorbents. From a literature survey, there are many studies that reported the CV dye adsorption from water using different adsorbent materials. In this study, C-HP gave a comparable high adsorption uptake and high adsorption efficiency of the adsorbent compared to the other adsorbent listed. As shown in Table 5, it is evident that the C-HP material demonstrated an excellent uptake capacity for CV dye removal compared with reported adsorbents. The q_m value evaluated shows that C-HP has the highest value compared the other adsorbents. For the other adsorbents each of them took a longer time in terms of contact time to achieve the adsorption capacity. Moreover, the maximum uptake capacity of C-HP increased significantly after treatment with H_2O_2. Thus, we conclude that the chemical treatment of C-HP may be a useful approach to improve the CV dye adsorption performance. Finally, the as-developed C-HP material can be recommended as a potential and inexpensive adsorbent to clean up CV dye from wastewaters.

Table 5: Comparison with other adsorbents.

Adsorbent	**Dye**	**Contact time (mins)**	**pH**	**q_m (mg/g)**	**q_e (mg/g)**	**Ref.**
Cellulose-Hydrogen Peroxide	CV	90	8	1428	837.5	This study
Sodium hydroxide-modified avocado shells (NaOH-AS)	CV	150	8	179.80	78.32	(Ait Haki et al. 2021)
agricultural rice bran waste	CV	60	10	600	404	(Rezazadeh et al. 2020)
Cellulose-Egyptian water hyacinth	CV	> 60	10	181.8	131.50	(Salahuddin et al. 2020)

Conclusion

In this study, it is proved that adsorbent C-HP was synthesized and characterized with ATR – FTIR, TGA and XRD. Adsorption result shows that C-HP can be efficiently used for crystal violet dye removal in aqueous solution. The removal capacity for CV was investigated systematically. Adsorption isotherm indicate that the adsorption behaviour was fitted to the Freundlich isotherm model. The maximum uptake for CV reached 1428.57mg/g, which much higher than the other adsorbents. These above findings suggest that C-HP could be used as a cost – effective and efficient adsorbent for removal of crystal violet dyes in aqueous solution.

Acknowledgements

This work was financially supported by the Universiti Teknologi Malaysia through RUG under PAS-DTD (R.J130000.8054.4J725).

References

Abdul Khalil, H. P. S., Bhat, A. H., & Ireana Yusra, A. F. (2012). Green composites from sustainable cellulose nanofibrils: A Review. Carbohydrate Polymers, 87(2), 963–979.

Abdullah, M. A., Nazir, M. S., Raza, M. R., Wahjoedi, B. A., & Yussof, A. W. (2016). Autoclave and ultra-sonication treatments of oil palm empty fruit bunch fibers for cellulose extraction and its polypropylene composite properties. Journal of Cleaner Production, 126, 686–697.

Acemioglu, B., & Alma, M. H. (2001). Equilibrium Studies on adsorption of cu(ii) from aqueous solution onto cellulose. Journal of Colloid and Interface Science, 243(1), 81–84.

Ait Haki, M., Imgharn, A., Aarab, N., Hsini, A., Essekri, A., Laabd, M., El Jazouli, H., Elamine, M., Lakhmiri, R., & Albourine, A. (2021). Efficient removal of crystal violet dye from aqueous solutions using sodium hydroxide-modified avocado shells: Kinetics and isotherms modeling. Water Science and Technology, 85(1), 433–448.

AL-Shehri, H. S., Almudaifer, E., Alorabi, A. Q., Alanazi, H. S., Alkorbi, A. S., & Alharthi, F. A. (2021). Effective adsorption of crystal violet from aqueous solutions with effective adsorbent: Equilibrium, Mechanism Studies and modeling analysis. Environmental Pollutants and Bioavailability, 33(1), 214–226.

Bachtiar, D., Sapuan, S. M., & Hamdan, M. M. (2008). The effect of alkaline treatment on tensile properties of sugar palm fibre reinforced epoxy composites. Materials & Design, 29(7), 1285–1290.

Beroual, M., Trache, D., Mehelli, O., Boumaza, L., Tarchoun, A. F., Derradji, M., & Khimeche, (2020). Effect of the delignification process on the physicochemical properties and thermal stability of microcrystalline cellulose extracted from date palm fronds. Waste and Biomass Valorization, 12(5), 2779–2793.

Chang, S. H. (2014). An overview of empty fruit bunch from oil palm as feedstock for bio-oil production. Biomass and Bioenergy, 62, 174–181.

Chin, S. X., Chia, C. H., & Zakaria, S. (2012). Production of reducing sugar from oil palm empty fruit bunch (EFB) cellulose fibres via acid hydrolysis. BioResources, 8(1).

Danish, M., Ahmad, T., Hashim, R., Hafiz, M. R., Ghazali, A., Sulaiman, O., & Hiziroglu, S. (2015). Characterization and adsorption kinetic study of surfactant treated oil palm (elaeis guineensis) empty fruit bunches. Desalination and Water Treatment, 57(20), 9474–9487.

Diakité, M., Paul, A., Jäger, C., Pielert, J., & Mumme, J. (2013). Chemical and morphological changes in hydrochars derived from microcrystalline cellulose and investigated by chromatographic, spectroscopic and adsorption techniques. Bioresource Technology, 150, 98–105.

dos Santos, A. B., Cervantes, F. J., & van Lier, J. B. (2007). Review Paper on current technologies for decolourisation of textile wastewaters: Perspectives for Anaerobic Biotechnology. Bioresource Technology, 98(12), 2369–2385.

Encyclopædia Britannica, inc. (n.d.). Dye. Encyclopædia Britannica. Retrieved January 22, 2022, from https://www.britannica.com/technology/dye

Fitriana, N. E., Suwanto, A., Jatmiko, T. H., Mursiti, S., & Prasetyo, D. J. (2020). Cellulose extraction from sugar palm (Arenga Pinnata) fibre by alkaline and peroxide treatments. IOP Conference Series: Earth and Environmental Science, 462(1), 012053.

Freundlich, H. (1906). *Über die Adsorption in Lösungen*. Zeitschrift für Physikalische Chemie, 57**,** 385–470.

Gnanasundaram, N., Loganathan, M., & Singh, A. (2017). Optimization and performance parameters for adsorption of cr6+ by microwave assisted carbon from Sterculia foetida shells. IOP Conference Series: Materials Science and Engineering, 206, 012065.

Gupta, V. K., Mittal, A., Jain, R., Mathur, M., & Sikarwar, S. (2006). Adsorption of safranin-T from wastewater using waste materials— activated carbon and activated Rice Husks. Journal of Colloid and Interface Science, 303(1), 80–8

Guo, Y., & Rockstraw, D. A. (2006). Physical and chemical properties of carbons synthesized from Xylan, cellulose, and Kraft lignin by H3PO4 activation. Carbon, 44(8), 1464–147

HAMDAOUI, O. (2006). Batch study of liquid-phase adsorption of methylene blue using cedar sawdust and crushed brick. Journal of Hazardous Materials, 135(1-3), 264–273.

He, Q., Wang, Q., Zhou, H., Ren, D., He, Y., Cong, H., & Wu, L. (2018). Highly crystalline cellulose from brown seaweed saccharina japonica: Isolation, characterization and microcrystallization. Cellulose, 25(10), 5523–5533.

Jayasantha Kumari, H., Krishnamoorthy, P., Arumugam, T. K., Radhakrishnan, S., & Vasudevan, D. (2017). An efficient removal of crystal violet dye from waste water by adsorption onto TLAC/Chitosan Composite: A novel low-cost adsorbent. International Journal of Biological Macromolecules, 96, 324–333

Jonoobi, M., Khazaeian, A., Tahir, P. M., Azry, S. S., & Oksman, K. (2011). Characteristics of cellulose nanofibers isolated from Rubberwood and empty fruit bunches of oil palm using chemo-mechanical process. Cellulose, 18(4), 1085–1095.

Kandisa, R. V., & Saibaba KV, N. (2016). Dye removal by adsorption: A Review. Journal of Bioremediation & Biodegradation, 07(06).

Khalil, H. P. S. A., Ismail, H., Rozman, H. D., & Ahmad, M. N. (2001). The effect of acetylation on interfacial shear strength between plant fibres and various matrices. European Polymer Journal, 37(5), 1037–1045.

Khezami, L., Chetouani, A., Taouk, B., & Capart, R. (2005). Production and characterisation of activated carbon from wood components in powder: Cellulose, lignin, Xylan. Powder Technology, 157(1- 3), 48–56.

Klemm, D., Heublein, B., Fink, H.-P., & Bohn, A. (2005). Cellulose: Fascinating biopolymer and sustainable raw material. Angewandte Chemie International Edition, 44(22), 3358–3393.

Kumar Gupta, P., Sai Raghunath, S., Venkatesh Prasanna, D., Venkat, P., Shree, V., Chithananthan, C., Choudhary, S., Surender, K., & Geetha, K. (2019). An update on overview of cellulose, its structure and applications. Cellulose.

Langmuir, I. (1917). *The constitution and fundamental properties of solids and liquids. Part I. Solids*. Journal of the American Chemical Society, 38**(**11), 2221–2295.

Li, B., Xu, W., Kronlund, D., Määttänen, A., Liu, J., Smått, J.-H., Peltonen, J., Willför, S., Mu, X., & Xu,

C. (2015). Cellulose nanocrystals prepared via formic acid hydrolysis followed by tempo- mediated oxidation. Carbohydrate Polymers, 133, 605–612.

Ling, Z., Wang, T., Makarem, M., Santiago Cintrón, M., Cheng, H. N., Kang, X., Bacher, M., Potthast, A., Rosenau, T., King, H., Delhom, C. D., Nam, S., Vincent Edwards, J., Kim, S. H., Xu, F., & French, A. D. (2019). Effects of ball milling on the structure of cotton cellulose. Cellulose, 26(1), 305–328.

Maekawa, M., Hashimoto, A., & Tahara, M. (2007). Effects of ph in hydrogen peroxide bleaching of cotton fabrics pretreated with ferrous sulfate. Textile Research Journal, 77(4), 222–226.

Mittal, A., Mittal, J., Malviya, A., Kaur, D., & Gupta, V. K. (2010). Adsorption of hazardous dye crystal violet from wastewater by waste materials. Journal of Colloid and Interface Science, 343(2), 463– 473.

Nazir, M. S., Wahjoedi, B. A., Yussof, A. W., and Abdullah, M. A. (2013). "Eco-friendly extraction and characterization of cellulose from oil palm empty fruit bunches," BioRes. 8(2), 2161- 2172.

O'Connell, D. W., Birkinshaw, C., & O'Dwyer, T. F. (2008). Heavy metal adsorbents prepared from the modification of cellulose: A Review. Bioresource Technology, 99(15), 6709–6724.

Ottoboni, S., Simurda, M., Wilson, S., Irvine, A., Ramsay, F., & Price, C. J. (2020). Understanding effect of filtration and washing on dried product: Paracetamol case study. Powder Technology, 366, 305–323.

Padzil, F. N., Lee, S. H., Ainun, Z. M., Lee, C. H., & Abdullah, L. C. (2020). Potential of oil palm empty Fruit Bunch Resources in nanocellulose hydrogel production for Versatile applications: A review. Materials, 13(5), 1245.

Pratap-Singh, A., Guo, Y., Lara Ochoa, S., Fathordoobady, F., & Singh, A. (2021). Optimal ultrasonication process time remains constant for a specific nanoemulsion size reduction system. Scientific Reports, 11(1).

Pinto, E., Aggrey, W. N., Boakye, P., Amenuvor, G., Sokama-Neuyam, Y. A., Fokuo, M. K., Karimaie, H., Sarkodie, K., Adenutsi, C. D., Erzuah, S., & Rockson, M. A. (2022).

Cellulose processing from biomass and its derivatization into carboxymethylcellulose: A Review. Scientific African, 15.

Rayung, M., Ibrahim, N. A., Zainuddin, N., Saad, W. Z., Razak, N. I. A., & Chieng, B. W. (2014, August 22). The effect of fiber bleaching treatment on the properties of poly(lactic acid)/oil palm empty fruit bunch fiber composites. International journal of molecular sciences.

Rezazadeh, M., Baghdadi, M., Mehrdadi, N., & Ali Abdoli, M. (2020). Adsorption of crystal violet dye by agricultural rice bran waste: Isotherms, kinetics, modeling and influencing factors. Environmental Engineering Research.

Roy, M., & Saha, R. (2021). Dyes and their removal technologies from wastewater: A critical review. Intelligent Environmental Data Monitoring for Pollution Management, 127–160.

Salahuddin, N., Abdelwahab, M. A., Akelah, A., & Elnagar, M. (2020). Adsorption of Congo red and crystal violet dyes onto cellulose extracted from Egyptian water hyacinth. Natural Hazards, 105(2), 1375–1394.

Sato, T., Mori, S., Septiyanti, M., Nakamura, H., Hongo, C., Matsumoto, T., & Nishino, T. (2020). Preparation and characterization of cellulose nanofiber cryogels as oil absorbents and enzymatic lipolysis scaffolds. Carbohydrate Research, 493, 108020.

Silvério, H. A., Flauzino Neto, W. P., Dantas, N. O., & Pasquini, D. (2013). Extraction and characterization of cellulose nanocrystals from Corncob for application as reinforcing agent in Nanocomposites. Industrial Crops and Products, 44, 427–436.

Sheltami, R. M., Abdullah, I., Ahmad, I., Dufresne, A., & Kargarzadeh, H. (2012). Extraction of cellulose nanocrystals from Mengkuang leaves (pandanus tectorius). Carbohydrate Polymers, 88(2), 772– 779.

Sisak, M. A., Daik, R., & Ramli, S. (2015). Characterization of cellulose extracted from oil palm empty Fruit Bunch. AIP Conference Proceedings.

Song, K., Zhu, X., Zhu, W., & Li, X. (2019). Preparation and characterization of cellulose nanocrystal extracted from Calotropis procera biomass. Bioresources and Bioprocessing, 6(1).

Suhas, Gupta, V. K., Carrott, P. J. M., Singh, R., Chaudhary, M., & Kushwaha, S. (2016). Cellulose: A review as natural, modified and activated carbon adsorbent. Bioresource Technology, 216, 1066–1076.

Tarchoun, A. F., Trache, D., Klapötke, T. M., Derradji, M., & Bessa, W. (2019). Ecofriendly isolation and characterization of microcrystalline cellulose from giant reed using various acidic media. Cellulose, 26(13-14), 7635–7651.

Wang, L., & Li, J. (2013). Adsorption of C.I. reactive red 228 dye from aqueous solution by modified cellulose from flax shive: Kinetics, equilibrium, and thermodynamics. Industrial Crops and Products, 42, 153–158.

Yu, H., Qin, Z., Liang, B., Liu, N., Zhou, Z., & Chen, L. (2013). Facile extraction of thermally stable cellulose nanocrystals with a high yield of 93% through hydrochloric acid hydrolysis under hydrothermal conditions. Journal of Materials Chemistry A, 1(12), 3938.

Zhang, K., Sun, P., Liu, H., Shang, S., Song, J., & Wang, D. (2016). Extraction and comparison of carboxylated cellulose nanocrystals from bleached sugarcane bagasse pulp using two different oxidation methods. Carbohydrate Polymers, 138, 237–243